N90-29045

Characterization and Control of Self-motions in Redundant Manipulators

J. Burdick*, H. Seraji†

Abstract

The presence of redundant degrees of freedom in a manipulator structure leads to a physical phenomenon known as a "self-motion," which is a continuous motion of the manipulator joints that leaves the end-effector motionless. In the first part of the paper, a global manifold mapping reformulation of manipulator kinematics is reviewed, and the inverse kinematic solution for redundant manipulators is developed in terms of self-motion manifolds. Global characterizations of the self-motion manifolds in terms of their number, geometry, homotopy class, and null space are reviewed using examples. Much previous work in redundant manipulator control has been concerned with the "redundancy resolution" problem, in which methods are developed to determine, or "resolve," the motion of the joints in order to achieve end-effector trajectory control while optimizing additional objective functions. Redundancy resolution problems can be equivalently posed as the control of self-motions. In the second part of the paper, alternatives for redundancy resolution are briefly discussed.

1. Introduction

A redundant manipulator is one that has more degrees of freedom than is the minimum number nominally required to perform a given set of tasks. Redundancy in the manipulator structure yields increased dexterity and versatility for performing a task due to the infinite number of joint motions which result in the same end-effector trajectory. However, this richness of joint motions complicates the manipulator control problem considerably. In order to take advantage of redundancy, control schemes which effectively utilize redundancy in some useful manner must be developed. In recent years redundant manipulators have been the subject of considerable research, and several uses for redundancy and methods to resolve redundancy have been suggested. Much of the research on redundant manipulators has been explicitly or implicitly based on the Jacobian pseudo-inverse approach [1] for the utilization of redundancy through *local* optimization of some criterion functional.

This paper presents a different approach to the kinematics of redundant manipulators, which is based on a manifold mapping reformulation that stresses *global*, rather than local, kinematic analysis. Within this framework, the infinite number of redundant manipulator inverse kinematic solutions are naturally interpreted as a finite set of "self-motion manifolds." The self-motion manifold approach is a useful foundation for studying redundant manipulator kinematics. Additionally, redundancy resolution can be equivalently posed as the control of self-motions; and the self-motion manifolds are useful for investigating, interpreting, and formulating both local and global redundancy resolution techniques.

The resolution of the redundancy can be implemented by direct control of a set of self-motion parameters, by direct control of a related set of user-defined kinematic functions, or through the optimization of an objective function. Redundancy resolution can also be posed as a local or global problem.

* Dept. of Mechanical Engineering, California Institute of Technology, Pasadena, CA

† Jet Propulsion Laboratories, California Institute of Technology, Pasadena, CA

2. Kinematics of Redundant Manipulators

A manipulator forward kinematic function, f, is a nonlinear vector function which relates a set of n joint coordinates, θ, to a set of m end-effector coordinates:

$$\mathbf{x} = f(\theta). \tag{1}$$

One of the primary problems of practical interest in manipulator kinematics is determining the set of solutions to the inverse kinematic function, f^{-1}:

$$\theta = f^{-1}(\mathbf{x}). \tag{2}$$

For non-redundant manipulators, there is a finite and bounded set of joint angles which satisfy (2). Each solution corresponds to a distinct manipulator "pose." For redundant manipulators, there are an infinite number of joint angles which satisfy the inverse kinematic relation in (2), although , as will be shown, the infinity of solutions can be grouped into a finite and bounded set of smooth manifolds.

Previous redundant manipulator investigations have often focused on the linearized first order instantaneous kinematic relation between end-effector velocities and joint velocities:

$$\dot{\mathbf{x}} = \mathbf{J}(\theta)\dot{\theta} \tag{3}$$

where $\mathbf{J}(\theta) = df(\theta)/d\theta$ is the $m \times n$ manipulator end-effector Jacobian matrix. When $n > m$, $\mathbf{J}(\theta)$ is not uniquely invertible, and pseudo-inverse techniques [1] can be used to select a joint velocity vector, from the infinity of possible solutions, which generates a desired end-effector velocity vector. In the redundant manipulator literature, the inverse solution to (3) is often referred to as the inverse kinematic solution, rather than (2).

The redundant degrees of freedom, which lead to multiply infinite solutions in (2) and (3), can be used to perform additional tasks or optimize manipulator kinematic, dynamic, or mechanical properties. The simplest inverse solution to (3) is based on the Jacobian pseudo-inverse:

$$\dot{\theta} = \mathbf{J}_W^{\dagger}(\theta)\ \dot{\mathbf{x}} \tag{4}$$

where $\mathbf{J}_W^{\dagger}(\theta) = W\mathbf{J}^T(\theta)[\mathbf{J}(\theta)W\mathbf{J}^T(\theta)]^{-1}$ is a weighted pseudo-inverse of the manipulator end-effector Jacobian matrix. W is a symmetric positive definite matrix, and the solution in (4) instantaneously minimizes the weighted quadratic form $\dot{\theta}^T W^{-1}\dot{\theta}$ at configuration θ. This solution can be modified by adding a null space component to the instantaneous joint velocities:

$$\dot{\theta} = \mathbf{J}_W^{\dagger}(\theta)\ \dot{\mathbf{x}} + (\mathbf{I} - \mathbf{J}_W^{\dagger}(\theta)\ \mathbf{J}(\theta))\mathbf{y} \tag{5}$$

where $\mathbf{y}$ is an arbitrary $n \times 1$ vector. The term $(\mathbf{I} - \mathbf{J}_W^{\dagger}(\theta)\ \mathbf{J}(\theta))$ projects $\mathbf{y}$ onto the null space of the manipulator Jacobian matrix. Physically, any motion in the null space is an *instantaneous* motion of the manipulator joints which causes no motion of the end-effector. Many redundancy resolution criteria can be developed as potential functions, and $\mathbf{y}$ can be the gradient of the resolution potential function, $g(\theta)$: $\mathbf{y} = \alpha\nabla g(\theta)$,where α is a scalar. Other instantaneous redundancy resolution techniques, including task optimization [9] have also been proposed.

The global inverse kinematic solution in (2) can be conveniently investigated by introducing a manifold mapping reformulation of manipulator kinematics which considers the aggregate, and thus *global*, action of the kinematic and inverse kinematic maps on the configuration space manifold. This approach allows simple topological tools to be applied to the study of manipulator kinematics [2]. The following sections present an overview of the manifold mapping

reformulation and the interpretation of redundant inverse kinematic solutions in terms of self-motion manifolds. This approach gives a natural interpretation to the solution to (2), offers useful insight into the local redundancy resolution schemes in (4) and (5), and suggests new approaches to redundancy resolution.

3. A Manifold Mapping Reformulation of Manipulator Kinematics

Only revolute jointed manipulators will be considered in this paper, although manipulators constructed from other lower pair joints can be similarly treated. In order to globally analyze manipulator kinematic functions it is useful to rephrase the forward and inverse kinematic problems in terms of manifold mappings. From a point-wise mapping perspective, the forward kinematic function in (1) maps a unique joint configuration, θ, to an end-effector location, $\mathbf{x}$: $\mathbf{x} = f(\theta)$. The set of all possible joint configurations forms a space, termed the "joint space" or "configuration space," which has a simple manifold structure. Similarly, the set of all possible end-effector locations forms the "workspace," which also has a manifold structure.

First consider how a manipulator configuration space can be developed as a manifold. Let θ_j denote the joint rotation angle for the j^{th} revolute joint. If the motion of the j^{th} joint is not limited due to mechanical stops, θ_j can take on all values in the interval $[-\pi, \pi]$. The identification of the two end-points of the interval, π and $-\pi$, yields a circle, denoted by the symbol S^1 in Figure 1. The configuration space, $\mathcal{C}$, of an n-revolute-jointed manipulator is a product space formed by the n-times product of the individual joint manifolds:

$$\mathcal{C} = S^1 \times S^1 \times \cdots \times S^1 = T^n \tag{6}$$

where T^n is an *n-torus*, which is a compact n-dimensional manifold. Each of the circles that make up the torus is termed a *generator* of the torus, and is physically equivalent to a 2π rotation of one joint. There is a one-to-one correspondence between each point in the n-torus configuration space manifold and a discrete manipulator configuration. For example, the $2R$ planar manipulator in Figure 2a has a 2-torus configuration space shown in Figure 2b.

While the torus geometry properly captures the topology of the configuration space manifold, there are times when other representations of the torus are useful. For example, the 2-torus representation of the $2R$ manipulator configuration space can be presented as a square with dimension 2π by "cutting" the torus along two generators, as shown in Figure 3. The 3-torus configuration space of a 3R manipulator can not be directly viewed in a 3-dimensional space, but it can be presented as a cube by cutting along the 3-tori generators, as in Figure 3. These configuration space representations are also useful for plotting trajectories and surfaces in θ-space, and all of the "cubes" in Figures 4 and 5 represent 3-tori.

To establish the geometry of the workspace, attach a frame to the manipulator end-effector. The manipulator's workspace manifold, $\mathcal{W}$, is the set of all possible locations and orientations of this frame as the manipulator joints are swept through all points of the configuration space. The geometric characterization of $\mathcal{W}$ is more complex than the torus characterization of the configuration space [2,4]. Briefly, the workspace has a "layered" or sheet-like structure.

The forward kinematic function can be viewed as a mapping of points from the configuration space to the workspace. More importantly, one can consider the action of the forward kinematic function as *the global rearrangement of the configuration space manifold to produce the workspace manifold*:

$$f(\theta)\colon \mathcal{C} \rightarrow \mathcal{W}. \tag{7}$$

Roughly speaking, the forward kinematic map "rips" the configuration space manifold apart into pieces; distorts each piece; and combines the distorted pieces to form $\mathcal{W}$. A more detailed description of this mapping can be found in [2,4].

4. Redundant Inverse Kinematic Solution: Self-Motion Manifolds

For non-redundant manipulators, the inverse kinematic solution (also termed a *preimage*) $f^{-1}(\mathbf{x})$ of a regular [1] end-effector location is a bounded set of discrete configurations. It is known [5] that a $6R$ manipulator with arbitrary geometry can have up to 16 inverse kinematic solutions.

Let $r = n - m$ be the relative degrees of redundancy. Since f is a smooth function operating on a compact manifold, $\mathcal{C}$, $f^{-1}(\mathbf{x})$ must be an r-dimensional submanifold of the configuration space [6] if $\mathbf{x}$ is a regular value. The preimage submanifold may actually be divided into several disjoint manifolds. Formally, let a redundant inverse kinematic solution be denoted as the union of one or more disjoint r-dimensional manifolds:

$$f^{-1}(\mathbf{x}) = \bigcup_{i}^{n_{sm}} M_i(\psi) \tag{8}$$

where $M_i(\psi)$ is the i^{th} r-dimensional manifold in the inverse kinematic preimage and $M_i(\psi) \cap M_j(\psi) = \emptyset$ for $i \neq j$. Each of the preimage manifolds can be physically interpreted as a "self-motion," which is a continuous motion of the manipulator joints that leaves the end-effector motionless.

> **Definition:** Each of the disjoint r-dimensional manifolds in the inverse kinematic preimage will be termed a *self-motion manifold.*

n_{sm} is the number of self-motions in the preimage of $\mathbf{x}$ (bounds on the value of n_{sm} will be reviewed in Section 5), and a given end-effector location may have more than one associated distinct self-motion. The multiply disjoint self-motions are akin to the distinct poses that make up non-redundant manipulator inverse kinematic solutions. Each M_i can be parametrized by a set of r independent parameters, $\psi = \{\psi_1, \cdots, \psi_r\}$, which can be thought of as generalized coordinates for the self-motions. For a given end-effector location there is a unique choice (up to isomorphism) of self-motion parameters. However, the choice of the self-motion parameter can vary in different well-defined regions of the workspace [2]. The self-motion manifolds are best illustrated using two examples: a planar 3R manipulator (Figure 4) which is redundant with respect to the position of its end-effector, and a 4R regional manipulator which is similar to an "elbow" manipulator (Figure 5).

The self-motion manifolds of the $3R$ manipulator can be computed as follows. Let ψ, which is the orientation of the third link relative to a fixed reference system, be the parameter describing the internal motion of the manipulator (there are other valid, useful, and physically meaningful choices for the self-motion parameter). For a given end-effector location, (x_{ee}, y_{ee}), and an arbitrary value of ψ, there are two possible sets of joint angles, $\{\theta_{1a}, \theta_{2a}, \theta_{3a}\}$ and $\{\theta_{1b}, \theta_{2b}, \theta_{3b}\}$, which can be determined by evaluating the following equations:

$$\begin{aligned}
R_2 &= \sqrt{x_{ee}^2 + y_{ee}^2 + l_3^2 - 2l_3(x_{ee}\cos\psi + y_{ee}\sin\psi)} \\
\alpha &= \text{atan2}(y_{ee} - l_3\sin\psi, x_{ee} - l_3\cos\psi) \\
\gamma &= \cos^{-1}\left(\frac{l_1^2 + l_2^2 - R_2^2}{2l_1 l_2}\right) \qquad \eta = \cos^{-1}\left(\frac{l_1^2 + R_2^2 - l_2^2}{2l_1 R_2}\right) \\
\{\theta_{1a}, \theta_{2a}, \theta_{3a}\} &= \{(\alpha + \eta), (\gamma - \pi), (\psi - \alpha - \eta - \gamma + \pi)\} \\
\{\theta_{1b}, \theta_{2b}, \theta_{3b}\} &= \{(\alpha - \eta), (\pi - \gamma), (\psi - \alpha + \eta + \gamma - \pi)\}
\end{aligned} \tag{9}$$

[1] A *regular point* of the map f is a discrete configuration, θ, for which $f(\theta)$ is not singular (the Jacobian of f remains full rank). A *regular value* is an end-effector location $\mathbf{x} = f(\theta)$ where θ is a regular point. A *critical point* is a configuration, θ, such that $f(\theta)$ is singular (the Jacobian of f loses rank). A *critical value* is an end-effector location $\mathbf{x} = f(\theta)$ where θ is a critical point.

where l_1, l_2, l_3 are the lengths of links 1, 2, and 3. As ψ is swept through its feasible range of $[-\pi, \pi]$, equations (9) will generate two 1-dimensional manifolds in the configuration space. These manifolds may remain separate for all values of ψ, in which case there are two disjoint self-motions, or the two branches may meet at two points (corresponding to the singularities of the non-redundant $2R$ planar manipulator subchain formed by links 1 and 2), to form one self-motion manifold. In this case, the solution in (9) becomes imaginary for some values of ψ.

Figure 4 shows the self-motion manifolds of this planar manipulator (embedded in the configuration space 3-torus) for two different locations of the end-effector. The inverse image of point 1 contains two distinct self-motion manifolds, while the inverse image of point 2 contains only one self-motion. [Note: the self-motion manifolds corresponding to point 1 are closed loops, but appear as non-closed curves because of the cubic 3-torus representation in Figure 4.] The two distinct self-motion manifolds in the preimage of point 1 physically correspond to "up elbow" and "down elbow" self-motions which are an analogous generalization of the "up elbow" and "down elbow" configurations of a non-redundant two-link manipulator. Self-motions can be thought of as a natural generalization of the non-redundant manipulator concept of "pose" to redundant manipulators. In both cases, the self-motion manifolds are diffeomorphic[2] to a circle. However, the preimage of point 1 contains a generator of the configuration space (a 2π joint rotation) while the other preimage does not. These two self-motion manifolds are not homotopic[3].

Now consider the more complicated $4R$ manipulator in Figure 5. The kinematic parameters of this arm (using the modified Denavit-Hartenberg convention as in [7]) are: $\alpha_0 = 0$; $\alpha_1 = \alpha_2 = \pi/2$; $\alpha_3 = -\pi/2$; $a_0 = a_1 = a_2 = 0$; $a_3 = a_4 = l$; $d_1 = d_2 = d_3 = d_4 = 0$. Let the self-motion parameter, ψ, be the angle between the plane containing the third and fourth links and the vertical plane passing through joint axis 1. The following equations compute four inverse kinematic solutions, $\{\theta_{1a}, \theta_{2a}, \theta_{3a}, \theta_{4a}\}, \{\theta_{1b}, \theta_{2b}, \theta_{3b}, \theta_{4a}\}, \{\theta_{1c}, \theta_{2c}, \theta_{3c}, \theta_{4b}\}, \{\theta_{1d}, \theta_{2d}, \theta_{3d}, \theta_{4d}\}$, given an end-effector location, $\mathbf{x} = (x_{ee}, y_{ee}, z_{ee})$, and a value for the self-motion parameter, ψ.

Define the following variables, which are purely functions of the end-effector location and the link length parameter, l.

$$
\begin{aligned}
R_2 &= \sqrt{x_{ee}^2 + y_{ee}^2}; & R_3 &= \sqrt{x_{ee}^2 + y_{ee}^2 + z_{ee}^2}. \\
\cos\beta &= x_{ee}/R_2; & \sin\beta &= y_{ee}/R_2 & \beta &= atan2(y_{ee}, x_{ee}). \\
\cos\xi &= R_2/R_3; & \sin\xi &= z_{ee}/R_3; & \xi &= atan2(z_{ee}, R_2). \\
\cos\gamma &= R_3/2l; & \sin\gamma &= (1/2l)\sqrt{4l^2 - R_3^2}; & \gamma &= atan2(\sin\gamma, \cos\gamma).
\end{aligned}
\tag{10}
$$

There are two unique values of θ_4 which satisfy the inverse kinematic function:

$$
\theta_{4a} = 2\gamma; \qquad \theta_{4b} = -\theta_{4a} \tag{11}
$$

[2] A smooth map $f: X \to Y$ (where X and Y are manifolds) is a diffeomorphism if it is one-to-one and onto, and $f^{-1}: Y \to X$ is smooth. X and Y are diffeomorphic if such an f exists.

[3] Two maps, $f_0: X \to Y$ and $f_1: X \to Y$ are homotopic if there exists a smooth map, $F: X \times I \to Y$ such that $F(x, 0) = f_o(x)$ and $F(x, 1) = f_1(x)$. In other words, f_0 can be deformed to f_1 through a smoothly evolving family of maps, and two self-motion manifolds are homotopic if one can be continuously deformed into the other continuously on the surface of the configuration space torus.

There are four unique values of θ_2 (two corresponding to each value of θ_4 in (12)):

$$\begin{aligned} \theta_{2a} &= \cos^{-1}[\sin\xi\sin\gamma - \cos\xi\cos\gamma\cos\psi] \qquad \theta_{2b} = -\theta_{2a} \\ \theta_{2c} &= \cos^{-1}[\sin\xi\sin\gamma + \cos\xi\cos\gamma\cos\psi] \qquad \theta_{2d} = -\theta_{2c}. \end{aligned} \tag{12}$$

There are four corresponding values of θ_1 which can be computed as follows:

$$\begin{aligned} \theta_{1a} &= \text{atan2}\left[\frac{-\sin\psi\cos\gamma}{\sin\theta_{2a}}, \frac{-(\cos\xi\sin\gamma + \sin\xi\cos\gamma\cos\psi)}{\sin\theta_{2a}}\right] \qquad \theta_{1b} = \theta_{1a} \pm \pi \\ \theta_{1c} &= \text{atan2}\left[\frac{\sin\psi\cos\gamma}{\sin\theta_{2c}}, \frac{(-\cos\xi\sin\gamma + \sin\xi\cos\gamma\cos\psi)}{\sin\theta_{2c}}\right] \qquad \theta_{1d} = \theta_{1c} \pm \pi \end{aligned} \tag{13}$$

Similarly, there are four corresponding values of θ_3 which can be computed as follows:

$$\begin{aligned} \theta_{3a} &= \text{atan2}\left[\frac{-\cos\xi\sin\psi}{\sin\theta_{2a}}, \frac{\sin\xi\cos\gamma + \cos\xi\sin\gamma\cos\psi}{\sin\theta_{2a}}\right] \qquad \theta_{3b} = \theta_{3a} \pm \pi \\ \theta_{3c} &= \text{atan2}\left[\frac{\cos\xi\sin\psi}{\sin\theta_{2c}}, \frac{\sin\xi\cos\gamma + \cos\xi\sin\gamma\cos\psi}{\sin\theta_{2c}}\right] \qquad \theta_{3d} = \theta_{3c} \pm \pi \end{aligned} \tag{14}$$

The inverse solution is real for all values of ψ in the range $[-\pi, \pi]$. The four distinct self-motions of this manipulator can be generated by continuously sweeping ψ through its 2π range for fixed (x_{ee}, y_{ee}, z_{ee}). Figure 6 shows the cubic representation of the projection of these four self-motions onto the θ_1-θ_2-θ_3 and θ_2-θ_3-θ_4 3-tori (for the case in which $l = 1.0$, $(x_{ee}, y_{ee}, z_{ee}) = (0.0, 1.0, 0.9)$).

5. Characterizations of the Self-Motion Manifolds and the Jacobian Null Space

A more detailed study of the number, geometry, and homotopy classes of self-motion manifolds can be found in [2,3]. Some of the relevant results are requoted here.

Theorem 1: *An n-revolute-jointed redundant manipulator can have no more self-motions than the maximum number of inverse kinematic solutions of a non-redundant manipulator of the same class. That is, for a fixed end-effector location, redundant spherical, regional, and spatial manipulators with an arbitrary number of revolute joints can respectively have as many as 2, 4, and 16 distinct self-motions.*

Theorem 2: *The self-motion manifolds of an n-revolute-jointed redundant manipulator are diffeomorphic to T^r, an r-dimensional torus.*

Theorem 1 says that manipulators with arbitrary geometry have an upper bound on the number of self-motions for a fixed end-effector location. Roughly speaking, Theorem 2 says that each self-motion manifold is a distorted r-dimensional torus lying in the n-torus configuration space. This result actually holds for non-redundant manipulators as well, since the inverse image must be a 0-dimensional torus, or a point.

Self motions which are homotopic to each other form a *homotopy class.* The notion of a homotopy class has previously been used in [8] to characterize different redundancy resolution paths. While an exact bound on the possible number of self-motion homotopy classes which exist for a given manipulator has not been rigorously determined:

Proposition 3: *An n-revolute-jointed ($n \geq 7$) spatial manipulator can have as many as $2^{(n-2)}$ different self-motion homotopy classes.*

Many redundancy resolution techniques employ the null space of the manipulator Jacobian. In [3] it is shown that the null space has a simple interpretation as the self-motion manifold tangent space.

Theorem 4: The null space of the Jacobian matrix, evaluated at a particular joint configuration, θ_o, is the tangent to the self-motion manifold at θ_o.

Theorem 4 is particularly useful for interpreting instantaneous redundancy resolution techniques, such as (4) and (5).

6. User-Defined Kinematic Functions and the Augmented Jacobian

Locally, the m end-effector coordinates and the r self-motion parameters constitute a set of generalized coordinates for a redundant manipulator. Due to the multiplicity of self-motions, there are multiple sets of these generalized coordinates in different subregions of the configuration space. While $\mathbf{x}$ and ψ are a valid set of generalized coordinates for control of the redundant manipulator, ψ is not always physically meaningful or the direct parameters of interest in performing a task.

It is often expedient to define r kinematic functions $\phi = \{\phi_1(\theta), \phi_2(\theta), \ldots, \phi_r(\theta)\}$ to reflect some *"additional task"* that will be performed with the manipulator redundancy. Each ϕ_i can be a function of the joint angles $\{\theta_1, \ldots, \theta_n\}$ and the link geometric parameters. The user-defined kinematic functions can, for example, be the coordinates of a point on the manipulator, or the angle of a link with respect to a fixed reference system. However, for the set $\{\mathbf{x}, \phi\}$ to constitute a proper set of generalized coordinates, the user-defined kinematic functions must be expressible as independent functions of ψ: $\phi = \{\phi_1(\theta(\psi)), \ldots, \phi_r(\theta(\psi))\}$.

Let us consider an augmented task vector comprised of the end-effector coordinates and the self-motion parameters, $\{\mathbf{x}, \psi\}$. This new set of generalized coordinates can be instantaneously related to the manipulator joint angles through the *basic augmented Jacobian*:

$$\begin{bmatrix} \mathbf{J} \\ \mathbf{J}_\psi \end{bmatrix} = \begin{bmatrix} d\mathbf{x}/d\theta \\ d\psi/d\theta \end{bmatrix}. \tag{15}$$

A set of generalized coordinates based on the end-effector coordinates and the user-defined kinematic function, $\{\mathbf{x}, \phi(\psi)\}$, can be instantaneously related to the joint coordinates through the *augmented Jacobian* of the form:

$$\begin{bmatrix} \dot{\mathbf{x}} \\ \dot{\phi} \end{bmatrix} = \begin{bmatrix} \mathbf{I} & 0 \\ 0 & \frac{d\phi}{d\psi} \end{bmatrix} \begin{bmatrix} \mathbf{J} \\ \mathbf{J}_\psi \end{bmatrix} \dot{\theta}. \tag{16}$$

The augmented Jacobian will be singular whenever the basic augmented Jacobian in (15) loses rank and/or when the matrix $d\phi/d\psi$ loses rank. Let us focus on the singularities of the basic augmented Jacobian since they are invariant to the particular selection of user-defined kinematic functions. A singularity of the augmented Jacobian will also cause the following matrix to lose rank:

$$\begin{bmatrix} \mathbf{J} \\ \mathbf{J}_\psi \end{bmatrix} \begin{bmatrix} \mathbf{J}^T & \mathbf{J}_\psi^T \end{bmatrix} = \begin{bmatrix} \mathbf{J}\mathbf{J}^T & \mathbf{J}\mathbf{J}_\psi^T \\ \mathbf{J}_\psi\mathbf{J}^T & \mathbf{J}_\psi\mathbf{J}_\psi^T \end{bmatrix}. \tag{17}$$

Since the matrix in (17) is square, a deficiency in its rank can be determined by investigating its determinant:

$$\det \begin{bmatrix} \mathbf{J}\mathbf{J}^T & \mathbf{J}\mathbf{J}_\psi^T \\ \mathbf{J}_\psi\mathbf{J}^T & \mathbf{J}_\psi\mathbf{J}_\psi^T \end{bmatrix} = \det(\mathbf{J}\mathbf{J}^T) \cdot \det[\mathbf{J}_\psi(\mathbf{I} - \mathbf{J}^\dagger\mathbf{J})\mathbf{J}_\psi^T] \tag{18}$$

There are three conditions which lead to zero determinant in (18). The basic augmented Jacobian will lose rank when $\mathbf{J}$ loses rank (condition 1). The augmented Jacobian will also lose rank when $\det[\mathbf{J}_\psi(\mathbf{I} - \mathbf{J}^\dagger\mathbf{J})\mathbf{J}_\psi^T] = 0$. This will occur when $\mathbf{J}_\psi$ is rank-deficient (condition 2). Since $(\mathbf{I} - \mathbf{J}^\dagger\mathbf{J})$ is the null space projection operator, the augmented Jacobian will also lose rank when one or more rows of $\mathbf{J}_\psi$ are orthogonal to the null space of $\mathbf{J}$. If the rows of $\mathbf{J}_\psi$ are orthogonal to the null space of $\mathbf{J}$, the the null space of $\mathbf{J}$ is in the null space of $\mathbf{J}_\psi$. Therefore, the augmented Jacobian will also lose rank when $N(\mathbf{J}) \cap N(\mathbf{J}_\psi) \neq \emptyset$, where $N(\mathbf{J})$ and $N(\mathbf{J}_\psi)$ are the null spaces of $\mathbf{J}$ and $\mathbf{J}_\psi$ (condition 3).

7. Alternatives for Redundancy Resolution

There are many alternative ways to implement redundancy resolution. Redundancy resolution can be effected by direct trajectory control of the manipulator generalized coordinates, $\{\mathbf{x}(t), \psi(t)\}$, or the related coordinates, $\{\mathbf{x}(t), \phi(t)\}$, throughout the motion. This approach can be used to achieve a desirable evolution of the robot configuration while working in a confined space, or to avoid workspace obstacles, kinematic singularities, or joint limits [10]. An adaptive configuration control scheme, such as [10], or an extension of the operational space method [11] can be used to directly control the manipulator in the task coordinates. The method outlined in [10] also permits inequality constraints on the user-defined functions, $\phi(t)$. Alternatively, the equivalent joint space trajectories can be computed as a function of the specified end-effector and self-motion trajectories: $\theta(t) = f^{-1}(\mathbf{x}(t), \psi(t))$, and joint based control can be used to servo the manipulator along the joint trajectories. Equations (9) and (10-14) are examples of inverse kinematic functions for redundant manipulators.

In another approach, redundancy can be used to optimize a desirable objective function. Let $g(\theta)$ denote a scalar objective function to be optimized with the redundant degrees of freedom. The criterion for optimizing $g(\theta)$ with the constraint $\dot{\mathbf{x}} = \mathbf{J}\dot{\theta}$ is:

$$B\frac{\partial g}{\partial \theta} = 0 \tag{19}$$

where B is an $r \times n$ matrix formed from r linearly independent rows of $(\mathbf{I} - \mathbf{J}^\dagger\mathbf{J})$. Equation (19) is the result used by Baillieul [9] in the Extended Jacobian Method. Other methods for optimizing $g(\theta)$ generally lead to Jacobian based methods, such as (4) and (5). However, by defining $\phi(\theta) = B\partial g/\partial\theta$, we can see that kinematic optimization can also be reformulated as a special case of trajectory tracking.

Redundancy resolution problems can be posed as either local or global problems. In local approaches, such as (4) and (5), the objective function is *instantaneously* optimized. In global approaches, a global measure of the objective function is optimized over the length of a trajectory.

Local methods suffer from two drawbacks, which can be illustrated by considering a redundancy resolution problem with fixed end-effector location. The goal is to find the configuration which maximizes an objective function. Assume that the manipulator starts with the end-effector at the proper location, but with a configuration which does not maximize the objective function. In the null space based approach of (5), an incremental change in joint angle position (which will move the manipulator closer to the optimal configuration) is computed by projecting the gradient of the objective function onto the null space. This operation is equivalent to a first order gradient search over the self-motion manifold. First order gradient searches are prone to finding *local*, rather than global, maximum. Second, the null space techniques can only optimize over a single self-motion manifold. The true optimal configuration might be contained in another disjoint self-motion manifold, and consequently can not be found by such a technique.

The concept of a self-motion manifold can be useful for developing other approaches to global redundancy resolution. Again consider the case of redundancy resolution for fixed end-effector location. Let $g(\theta)$ be the objective function. For fixed end-effector location, θ is implicitly a function of ψ. Global redundancy resolution is then equivalent to finding:

$$\max_i \left(\max_\psi g_i(\psi) \right) \qquad (i = 1, \cdots, n_{sm}) \tag{20}$$

where $g_i(\psi)$ is the restriction of $g(\psi)$ to the i^{th} self-motion manifold. The local maxima and minima of the resolution function can be found as the roots to n_{sm} polynomials:

$$\frac{dg_i(\psi)}{d\psi} = 0 \qquad (i = 1, \cdots, n_{sm}). \tag{21}$$

the globally optimal solution is selected by evaluating $g(\psi)$ at each of the locally optimal roots to equations (21). Once the optimal set of self-motion parameters has been determined, the corresponding configuration, $\theta_{optimal}$, can be computed from the inverse kinematic function. To extend this approach to redundancy resolution along a trajectory, the polynomial equations could be solved along the path, and the multiple trajectories compared to determine the globally optimal one.

9. Conclusions

Self-motions are inherent in redundant manipulators, and understanding their characterization and control is important for establishing useful redundancy resolution techniques. This paper reviews a global manifold mapping reformulation of manipulator kinematics in which self-motions are naturally interpreted as sub-manifolds of the configuration space. Ways to characterize these self-motion manifolds are presented. Redundancy resolution techniques can be naturally reformulated and reinterpreted in terms of self-motion manifolds, rather than the Jacobian null space. This approach yields useful global insight into redundancy resolution.

9. Acknowledgements

The first author gratefully acknowledges the support of the System Development Foundation for part of this work, and many helpful comments from Professor Bernard Roth, Dr. Madhu Raghavan, and Dr. Charles Wampler. This research was performed in part at the Jet Propulsion Laboratory, California Institute of Technology, under contract with the National Aeronautics and Space Administration.

10. References

[1] C.A. Klein and C.H. Huang, "Review of the Pseudoinverse for Control of Kinematically Redundant Manipulators," *IEEE Transactions on Systems, Man and Cybernetics*, March, 1983.

[2] J. W. Burdick, "Kinematic Analysis and Design of Redundant Robot Manipulators," Ph.D. Thesis, Department of Mechanical Engineering, Stanford University, March 1988. To be issued as Stanford C.S. Report No. STAN-CS-88-1207.

[3] J. W. Burdick, "On the Inverse Kinematics of Redundant Manipulators: Characterization of the Self-Motion Manifolds," to appear in the proceedings of the *IEEE Robotics and Automation Conference*, Scottsdale, AZ, May, 1989.

[4] J. W. Burdick, "On the Kinematics of Redundant Manipulators: a Global Mapping Approach," in preparation.

[5] E.J.F. Primrose, "On the Input-Output Equations of the General 7R-Mechanism," *Mechanism and Machine Theory*, Vol. 21, No. 6, pp. 509-510, 1986.

[6] V. Guillemin and A. Pollack, *Differential Topology*, Prentice-Hall, Inc., Englewood Cliffs, New Jersey, 1974.

[7] J.J. Craig, *Introduction to Robotics: Manipulation and Control*, Addison-Wesley, Reading, Mass, 1986.

[8] J. Baillieul and D.P. Martin, "Issues in the Control of Kinematically Redundant Mechanisms," Proceedings of the *NATO Workshop on Redundancy in Robotics: Sensing, Design, and Control*, Salo, Italy, June 26-July 1, 1988, Springer Verlag.

[9] J. Baillieul, "Kinematic Programming Alternatives for Redundant Manipulators," *Proceedings of the IEEE International Conference on Robotics and Automation*, St. Louis, MO, March 25-28, 1985, pp. 722-728.

[10] H. Seraji, "Configuration Control of Redundant Manipulators," *Proceedings of the NATO Advanced Research Workshop on Robots with Redundancy: Design, Sensing, and Control*, Salo, Italy, June 26-July 1, 1988, Springer-Verlag.

[11] O. Khatib, "Dynamic Control of Manipulators in Operational Space," Sixth CISM-IFToMM Congress on the Theory of Mechanisms and Machines, New Delhi, India, Dec. 15-20, 1983, pp. 1128-1131.

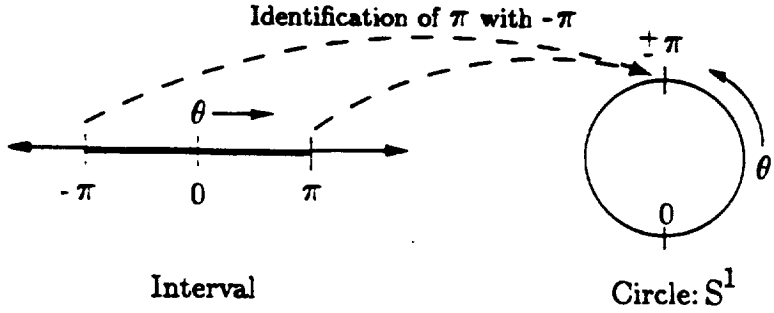

Figure 1: Revolute Joint Configuration Space Manifold

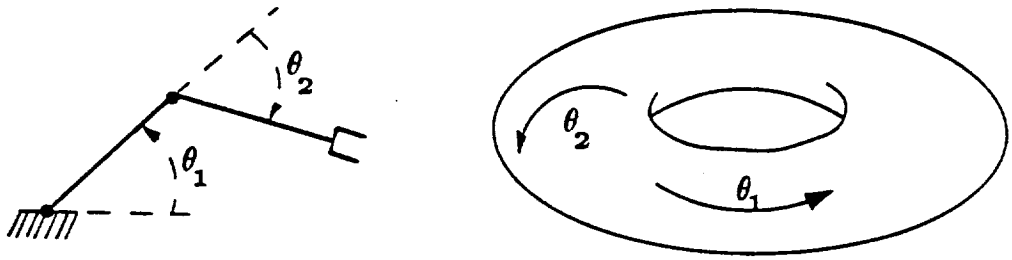

(a) Planar 2R Manipulator (b) 2-torus Configuration Space Manifold

Figure 2: Configuration Space of a $2R$ Manipulator

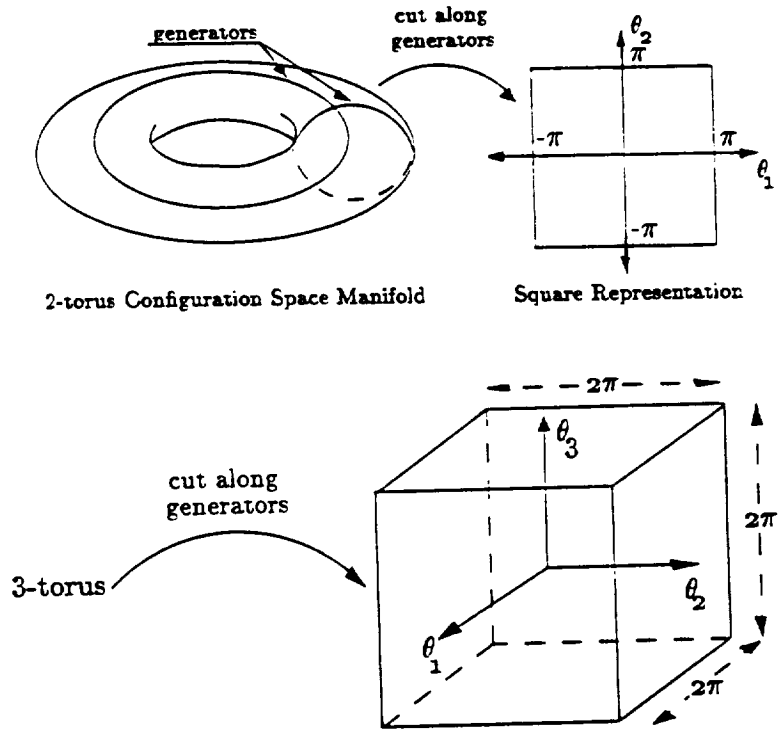

Figure 3: Square and Cube Representation of a 2-torus and 3-torus

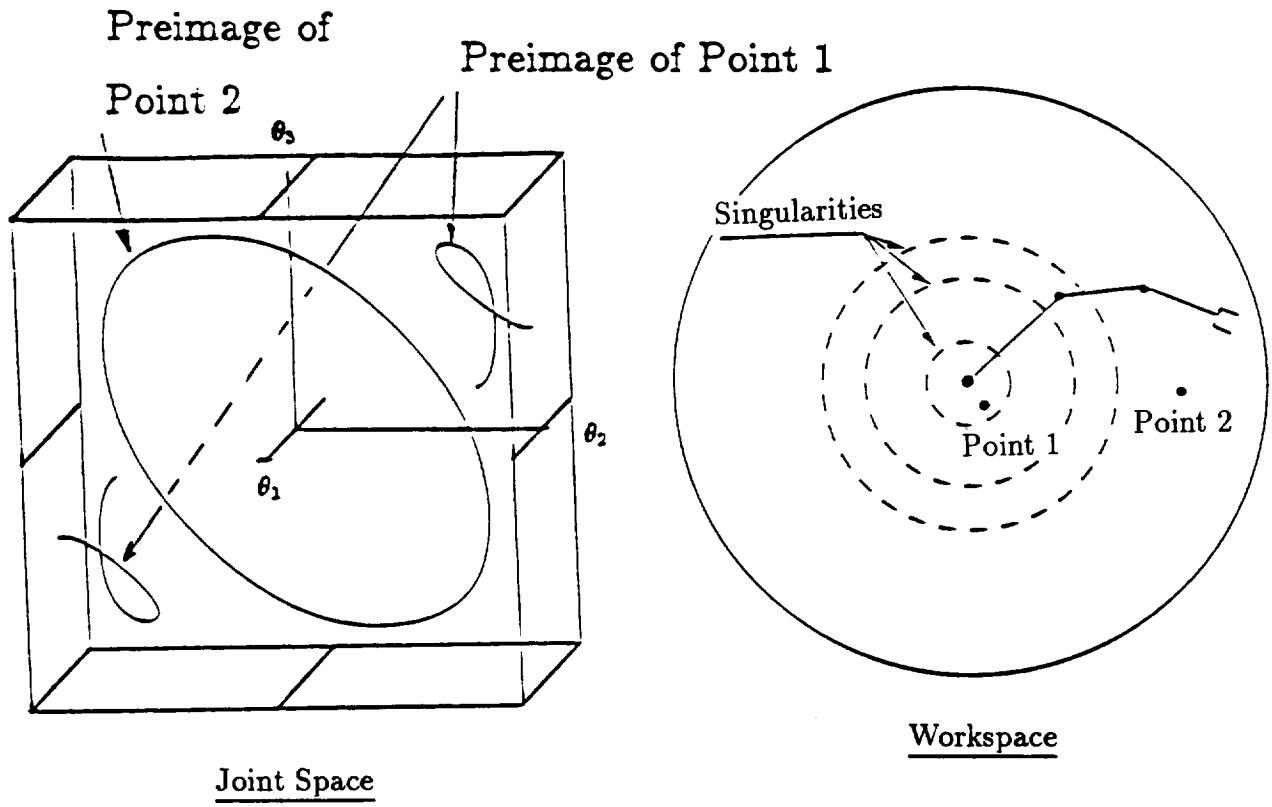

Figure 4: Self-Motion Manifolds for Two Regular Values in the Workspace of a $3R$ Planar Manipulator

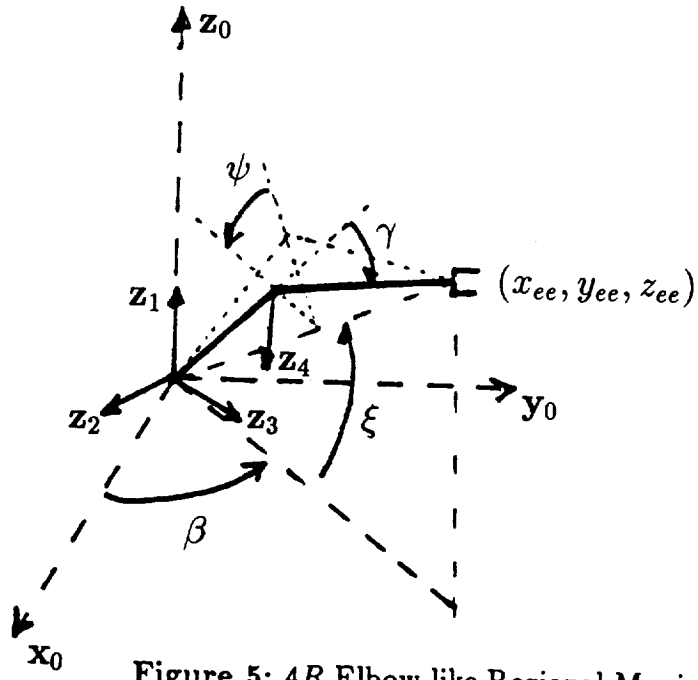

Figure 5: $4R$ Elbow-like Regional Manipulator

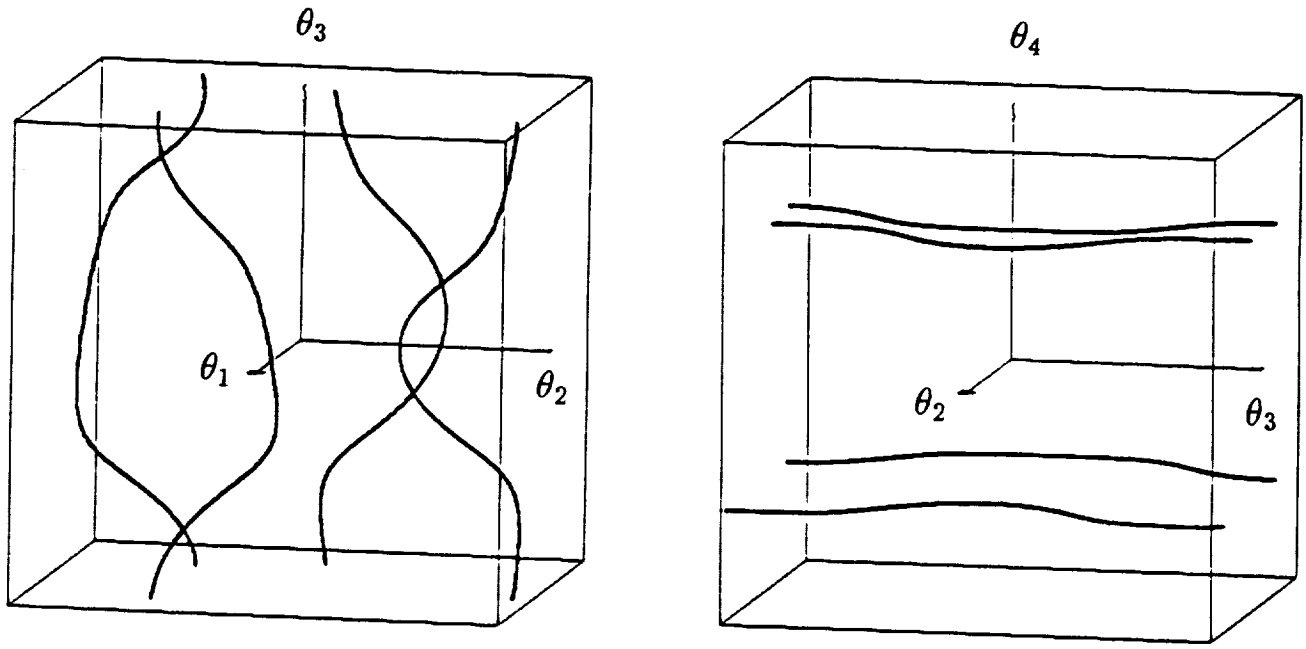

Projection onto θ_1-θ_2-θ_3 torus

Projection onto θ_2-θ_3-θ_4 torus

Figure 6: $4R$ Elbow-like Manipulator Self-Motion Manifolds